Physical Science International Journal

Volume 28, Issue 6, Page 21-34, 2024; Article no.PSIJ.124431
ISSN: 2348-0130

Investigating the Anisotropic Mechanical Behaviour of Steel Fibre-Reinforced Aluminium-Base Composites

Adeolu J. Alawode [a,b*], Shade O. Ademokoya [b,c], Ademola Bakare [b] and Olanrewaju Aina [b]

[a] Department of Petroleum Engineering, University of Ibadan, Ibadan (Post Code: 200221), Nigeria.
[b] Formerly of Department of Mechanical Engineering, University of Ado-Ekiti, Ado-Ekiti, Nigeria.
[c] School of Engineering, Babcock University, Ilishan-Remo, Nigeria.

Authors' contributions

This work was carried out in collaboration among all authors. All authors read and approved the final manuscript.

Article Information

DOI: https://doi.org/10.9734/psij/2024/v28i6856

Open Peer Review History:
This journal follows the Advanced Open Peer Review policy. Identity of the Reviewers, Editor(s) and additional Reviewers, peer review comments, different versions of the manuscript, comments of the editors, etc are available here: https://www.sdiarticle5.com/review-history/124431

Original Research Article

Received: 02/08/2024
Accepted: 04/10/2024
Published: 21/10/2024

ABSTRACT

Base metals are often reinforced with fibres to improve their mechanical behaviour; however, it is imperative to decide the range of fibres orientation that would yield favourable strength. In this work, using sand casting method, aluminium is reinforced with galvanized steel fibres at different orientations with the aim of investigating the anisotropic mechanical behaviour of the composites. The fibre orientations considered are 0°, 30°, 60° and 90°; while the mechanical properties evaluated are impact energy, tensile, compressive and fatigue properties. Unreinforced aluminium exhibits impact energy, elongation-at-fracture, ultimate tensile strength, and maximum compressive

**Corresponding author: E-mail: adelawode@yahoo.com;*

Cite as: *Alawode, Adeolu J., Shade O. Ademokoya, Ademola Bakare, and Olanrewaju Aina. 2024. "Investigating the Anisotropic Mechanical Behaviour of Steel Fibre-Reinforced Aluminium-Base Composites". Physical Science International Journal 28 (6):21-34. https://doi.org/10.9734/psij/2024/v28i6856.*

strength of 5.15 J, 15.88%, 72.56 MN/m^2, and 231.13 MN/m^2, respectively. With deviation of composite fibre orientation from 0° to 30°, 60° and 90°, impact energy decreases from 8.68 to 5.56, 4.75 and 4.61 J; elongation-at-fracture decreases from 24.58 to 17.91, 12.20 and 11.87%; ultimate tensile strength decreases from 132.70 to 89.17, 63.67 and 60.34 MN/m^2; and maximum compressive strength decreases from 310.66 to 251.06, 226.91 and 209.93 MN/m^2. At fatigue stress amplitude of 850 MN/m^2, the fatigue life of unreinforced specimen is 26 numbers of cycles-to-failure; while the deviation of composite fibre orientation from 0° to 30°, 60° and 90° yielded reduction in fatigue life from 64 to 36, 20 and 14 numbers of cycles-to-failure. Also, reduction in fatigue stress amplitude was found to increase the fatigue life of the specimens. The fatigue limit (or endurance limit) of unreinforeced specimen, and composite specimen having 0°, 30°, 60° and 90° fibre orientations are found to be 40, 70, 45, 35 and 25 MN/m^2, respectively; and the corresponding fatigue life are observed to be 35480, 199518, 112195, 10021 and 5297 numbers of cycles-to-failure, respectively. The findings in this work show that specimens with 0° fibre orientation have the highest endurance of deformation before fracture, followed by specimens with 30° fibre orientation, unreinforced specimens, specimens with 60° fibre orientation and specimens with 90° fibre orientation. This could be attributed to the fact that 0° fibre orientation offers continuous reinforcement spanning the longitudinal axis of the specimens, while fibre orientation from 30° to 90° offer areas of different degrees of shear stress concentration at fibre-matrix contacts aiding fibre-matrix debonding and crack propagation. In conclusion, this work shows that orientation of steel fibre reinforcement in aluminium matrix could be varied to achieve ranges of mechanical properties and performance needed for different practical applications.

Keywords: Anisotropic mechanical behaviour; steel fibre reinforcement; aluminium composites.

1. INTRODUCTION

In practical terms, no single material in nature can exhibit all the properties required of a typical engineering material. Therefore, alloys and composites are developed or manufactured by combining two or more materials having distinct properties with the aim of obtaining, through a synergy of properties of the different materials, an improved and unique behaviour for practical applications. These materials have the capacity of withstanding operating conditions ranging from very cold to super-high temperatures and extremely severe weathers. Alloys composed of materials combined metallurgically i.e., the constituent materials dissolve or blend into each other such that they do not remain distinct on the macroscopic level within the finished structure. However, composites are made of materials which remain distinct on the macroscopic level. Monolithic metals are often strengthened by reinforcement with particles and fibres via casting (to obtain metal matrix composites - MMCs) or with windings of resin-impregnated fibre strands (filaments) on its surface. The components of a composite material are: (i) the matrix as the continuous phase; (ii) the reinforcements; and (iii) the matrix-reinforcement interface. Mono-filament wires or fibres display a continuous reinforcement in the matrix while whiskers, short fibres and particles exhibit discontinuous/dispersed reinforcement in the matrix. The components can be metals only, non-metals only or combination of metal and non-metals such as polymers.

Composite materials have wide applications in engineering fields (such as construction of structures, buildings, bridges, panels, automotive, etc.) where stiffness, strength, hardness, temperature performance, and other mechanical properties are needed. Monolithic metals such as aluminium, magnesium, nickel, titanium, and cobalt can be used as metal matrix. Based on the needed applications and uses, other examples of composites are ceramic-matrix composites (CMCs), polymer-matrix composites (PMCs), carbon-carbon composites (CCCs) and hybrid composites (HCs). Some of the factors that influence the mechanical behaviour of composites are the size and shape of reinforcement, concentration of reinforcement, distribution and orientation of reinforcement, and volume fraction.

Of all the non-ferrous metal used for engineering applications, aluminium is the most widely used (especially in automotive engines, high-speed machinery, aircrafts and spacecrafts) because of its unique combination of properties; good corrosion resistance, high strength stiffness to weight ratio, good electrical and thermal conductivities, and advantages of recycling at low energy costs [1-3].

Extensive studies had been conducted on improving the mechanical properties of base metals including aluminium by alloying [4-6], heat treatment [7-11], particles reinforcement [12-16] and surface filament windings [17-19]. Also, literature had shown that metal matrix reinforcement with fibres offers potentials of improving the mechanical behaviour of base metals including aluminium.

The damage initiation and growth in fibre reinforced metal matrix composites had been studied [20]. Findings from test and analysis showed the differences between strength and fatigue failure modes in reinforced aluminium matrix composites (AMC) and those in titanium matrix composites (TMC).

Also, the thermoelastic response of metal matrix composites with large-diameter fibres subjected to thermal gradients had been investigated [21]. In contrast to previous micromechanical theories (that utilized classical homogenization schemes in the course of calculating microscopic and macroscopic field quantities) for the response of heterogeneous metal matrix composites subjected to thermal gradients, the study presented an approach that explicitly coupled actual microstructural details with the macrostructure of the composite. The study showed that the classical approach overestimated macroscopic field quantities, while the new approach generated favourable stress distributions by suitably modifying the internal microstructure of the composite.

The effect of fibre orientation on fatigue crack propagation in SCS-6/Ti-15-3 composites had been studied [22]. The fatigue crack at different angle of propagation in SCS-6/Ti-15-3 laminates at room temperature was studied. The maximum applied stress intensity was of the range of 20 to 30 $MPam^{1/2}$. The rates of fatigue crack growth at various applied stress intensity levels were measured and attributing mechanisms were discussed. Fatigue crack damage in angle-ply SCS-6/Ti-15-3 laminates was found to be much more complex than that observed in the unidirectional laminates. Synergy of the primary crack (originating from the notch) and secondary cracks resulted in remarkable failure of the laminate.

The dry sliding wear of a nickel-coated non-graphitic carbon fibres-reinforced A356 aluminium alloy was investigated [23]. Wear tests were carried out at constant load levels within the range of 5 to 300 N using a constant sliding velocity of 0.5 m s^{-1}. Wear behaviour of the fibre-reinforced and unreinforced A356 alloys, a particle-reinforced A356-20%SiC_p composite and a A30 grade grey cast iron (a conventional tribological material for automotive applications) were correlated. The reinforced A356-4%C_f was found to have higher wear resistance than the unreinforced A356 alloy in the mild wear regime. This was attributed to the improved load carrying capacity rendered by the carbon fibres coupled with the Al_3Ni inner-metallic precipitates formed during the fabrication process. Within the mild wear regime, the wear rates of the grey cast iron were observed to be remarkably higher than those of the composites possibly due to the surface and subsurface fracture initiated at graphite flakes.

Fatigue test was conducted on a unidirectional, ceramic fiber reinforced titanium matrix composite (SCS-6/Ti-15-3) at elevated temperature of 427°C with a view to characterizing the effects of loading ratio (i.e. stress and strain ratios) on the fatigue life and damage mechanisms [24]. At the maximum strain, most severe damage and shortest fatigue life were observed to occur under the fully reversible condition. fatigue life was found to increase as the strain ratio increased (i.e. as strain range decreased). However, the fatigue life under the strain-controlled mode was longer than under the load-controlled mode.

Also, the microstructures and mechanical properties of engineered short fibre-reinforced aluminium matrix composites fabricated using squeeze casting method was investigated [25]. Sintering, phosphoric acid treatment, phosphoric acid/aluminium hydroxide treatment, and infiltration with alumina powder and sintering were used in creating fibre junctions in a planar random alumina fibre array. Findings from microstructural analysis and mechanical properties evaluation showed that very low composite strength and ductility were obtained using phosphoric acid solution as compared to those of the as-received specimens. This is attributed to the chemical reaction-induced damage of the fibres. The phosphoric acid/aluminium hydroxide treatment yielded higher tensile strength as compared to the uniform fibre-reinforced composites without compromising the ductility and elastic modulus.

An overview of the tribological behaviour of aluminium metal matrix composites reinforced

with hard particles, short fibers, and solid lubricants was done [26]. The various technologies for producing automotive parts from these composites were also reviewed.

Composite development using aluminium alloy and carbon preforms using squeeze infiltration technique was investigated and presented with systematic design and synthesis method [27]. Optical and scanning electron microscopic studies were done on the specimens; proper infiltration, better distribution of fibers in matrix and an improved fibre-matrix bonding were observed. From the findings of Charpy Impact Test, the toughness of the composites yielded a four-fold improvement as compared with squeeze cast specimens.

Also, the mechanical properties of aluminium-based composites reinforced with steel fibres of 0^o (i.e., longitudinal) and 90^o (i.e., transverse) orientations were evaluated [28]. Unreinforced, longitudinal and transverse fibre-reinforced specimens displayed percentage elongation-at-fracture of 12,75, 27.50 and 11.00%, respectively; ultimate tensile strength of 83.51, 96.75 and 66.71 MNm^{-2}, respectively; impact energy of 47.80, 51.20 and 45 00 Nm, trespectively; and fatigue life of 209, 458 and 16 number of cycles-to-failure. The trends of the findings were attributed to the fact that longitudinal fibres offer resistance to deformation, while transverse fibre-matrix contacts assist cracks initiation and extension.

Glass fibre reinforced sandwich panels where plastics were bonded with thin aluminium sheets on either side with varying degrees of aluminium thickness fractions, fibre volume fractions and orientation in the layer was developed [29]. Impact performance was then investigated. The laminated sandwich panel was found to exhibit belter impact performance than base-aluminium; also, panel with cross-ply fibre orientation was observed to display better performance than unidirectional fibre orientation while increase in aluminium thickness and fibre volume was found to improve impact strength of the laminated panel.

The effect of heat treatment at 1350^oC on mechanical and wear characterization of coconut ash and E-glass fibre-reinforced aluminium hybrid composites was studied [30]. The hybrid aluminum alloy composites were made using stir-casting method. Hardness, wear and tensile tests were carried out with and without heat treated composites specimens. Addition of coconut ash and E-glass fibre was found to increase hardness and tensile strength of the composite but reduce the wear rate.

Also, the characteristics of reinforced hybrid composite of A6061/(Glass Fibre+Al_2O_3+SiC+B_4C) prepared through STIR casting were investigated [31]. An hybrid low-cost and light-weight composites with better strength, corrosion and wear resistance than the base metal was produced. Reinforcement was found to increase the strength but reduce the weight of the composites as compared to the unreinforced specimens.

The mechanical properties of aluminium wire reinforced polymer-carbon metal laminates were studied [32]. Aluminium wire reinforced polymer composite was made using hand lay-up method. Tensile strength, flexural and impact strength were evaluated. Carbon fibre reinforced polymer was observed to have more tensile, flexural and impact strength than the conventional carbon fiber and glass fiber composites; it was thus established that addition of aluminium wire mesh in carbon composites improves the mechanical properties.

The mechanical properties of carbon fiber reinforced aluminium metal matrix composite were investigated [33]. Uncoated continuous long spool-type pitch-based carbon fibers of 5 and 10 wt % were used in reinforcing AA 6061 aluminium base metal. The mechanical properties and morphological characteristics of the base (unreinforced) and reinforced aluminium specimens were studied.

The tensile and fatigue properties of fiber-reinforced metal matrix composites Cf/5056 Al were studied [34]. The mechanical properties of the reinforced metal matrix composites were observed to be highly dependent on fibers directions. The longitudinal fiber direction exhibited high strength and fatigue resistance than the tramverse fiber direction. Medium-strength interface combination was accounted to likely be responsible for the difference in fatigue damage mechanisms of Cf/5056Al composites under tension-tension and tension-compression loads, and the closeness of fatigue life curves.

The mechanical properties of jute fibre reinforced with aluminium oxide fortified epoxy composite were investigated [35]. The mechanical properties evaluated were tensile modulus,

tensile stress, percentage increase in weight, flexural stress and flexural modulus. The optimised tensile strength, flexural stress, tensile modulus and Flexural modulus of 43.49 MPa, 73.47 MPa, 4782.00E-3 and 6483.52E-3 GPa, respectively. Multiple performance index was determined using a hybrid grey-based adaptive neuro-fuzzy inference system (ANFIS) model. After validation, the constructed model was established to be capable of accurately predicting the required performance measure.

A study compared the mechanical properties of fiber-reinforced composite, high-strength steel and aluminum from experimental and numerical modeling approaches [36]. Experimental validation tests under uniaxial tensile loading showed a good correlation with finite element analysis predictions for carbon fiber reinforced thermoset polymer composites, DP600 steel and aluminum alloys (AC170 and 5754 series). The findings showed that the range of strain rate used had no remarkable influence on the strength of the composite materials.

However, with reference to the research work that evaluated the mechanical properties of aluminium composites having steel fibres of 0^o and 90^o orientations [28], the present work was motivated by the fact that analyzing the anisotropic mechanical behaviour of the composites would be more accurate if closer fibre orientations (such as 0°, 30°, 60°, and 90°) are considered. Also, the mechanical properties evaluated in this work include maximum compressive strength.

2. MATERIALS AND METHODS

2.1 Materials

The materials used in this study are aluminium alloy scraps (obtained from aluminium electric cables (E9VE) and internal combustion engine parts of motorcycles) and rigid galvanized steel fibre preforms for reinforcement. The reinforcing steel fibre is of 0.55 mm diameter with a minimum breaking load of 6.18 KN. The steel fibres were purchased in Ado-Ekiti, Nigeria.

2.2 Fabrication of Steel Fibre Preforms

Four pieces of softwood were cut and divided into 2 pairs. The X-Y-Z dimensions of the longer pair are $10 \times 15 \times 295$ mm while those of shorter pair are $10 \times 15 \times 190$ mm. The shorter pair was evenly perforated. The woods were joined to form a rigid rectangular frame. A unidirectional reinforcing steel fibres arrangement through holes in the softwood (pair B) was done to obtain a rigid steel fibre preform.

2.3 Drag and Cope Assembly

A rectangular wooden slab was cut, its X-Y-Z dimensions are $205 \times 25 \times 305$ mm and it was perfectly surface finished with sand paper to obtain the shape of the pattern needed for a cavity in sand mould assembly of drag and cope. Foundry sand (consisting of silica sand, coal-dust, clay and starch that were mixed with the right proportion of water) was prepared. A drag was filled with the foundry sand and properly rammed. The wooden slab was pressed (but not totally submerged) into the drag. Parting sand was sprinkled on the drag surface to enhance the separation of drag and cope surfaces. The cope was properly aligned on the drag, and it was filled with the moulding sand and properly rammed.

Thereafter, the cope was separated from the drag, the pattern was removed leaving a mould cavity, and the drag and cope were allowed to dry naturally. A gating system for sprue and riser pins that would allow flow of molten metal was incorporated in the cope. The drag and cope were then assembled to allow the passage of molten metal to be poured in.

For unreinforced aluminium, the mould cavity was empty; however, the rectangular steel fibres preform was placed in the mould cavity in another drag and cope assembly to obtain fibre-reinforced aluminium composite.

2.4 Casting

The aluminium wires and scraps were cut to pieces and melted in a furnace at 750 ^oC for 30 minutes. Before casting, prevention of pores in the cast aluminium must be ensured. Therefore, a degassing flux tablet was lowered into the base of the molten aluminium using a steel plunger. With this, hydrogen bubbles with other impurities moved to the surface of the molten aluminium and were removed. The melting pot was then removed from the furnace, and the molten aluminium was poured into the mould cavity through the sprue until the cavity was filled up as gauged by the riser. About an hour after casting, the drag and cope assembly was shaken-out to remove a rectangular aluminium slab. The cast slabs were then surface-finished to obtain clean and smooth surface.

2.5 Test Specimens Machining

The rectangular cast unreinforced aluminium slab was machined to impact, tensile, compression, and fatigue test specimens. Also, the rectangular cast aluminium composite slabs was cut along different directions to obtain specimens having different fibre orientations with respect to direction of test. The fibre orientations achieved are 0° (i.e., axial or longitudinal direction), 30°, 60° and 90° (i.e., transverse direction).

As shown in Fig. 1, the tensile test specimen has a gauge length and diameter of 27 and 5 mm, respectively (Fig. 1a), the fatigue test specimen has a gauge length and central diameter of 24 and 5 mm, respectively (Fig. 1b), while the compression test specimen has gauge length and diameter of 25 and 8 mm, respectively (Fig. 1c). However, the impact specimen (Fig. 1d), with gauge length and diameter of 70 and diameter of 8 mm, respectively was notched at an angle of 45^{o} to a depth of 2 mm at the middle of the gauge length.

For each test specification, two similar specimens were machined with the aim of finding average values of mechanical properties.

2.6 Impact Test

An Izod Impact Testing Machine was used in determining the impact energy of the specimens; ASTM E602-91 standard was observed. The respective specimen was fixed on the machine as simple beam with the opposite face of the notch fixed to receive the hammer blow. The impact strength of a specimen was determined from the energy absorbed when the specimen was hit and deformed by a swing hammer of the machine released from a fixed height.

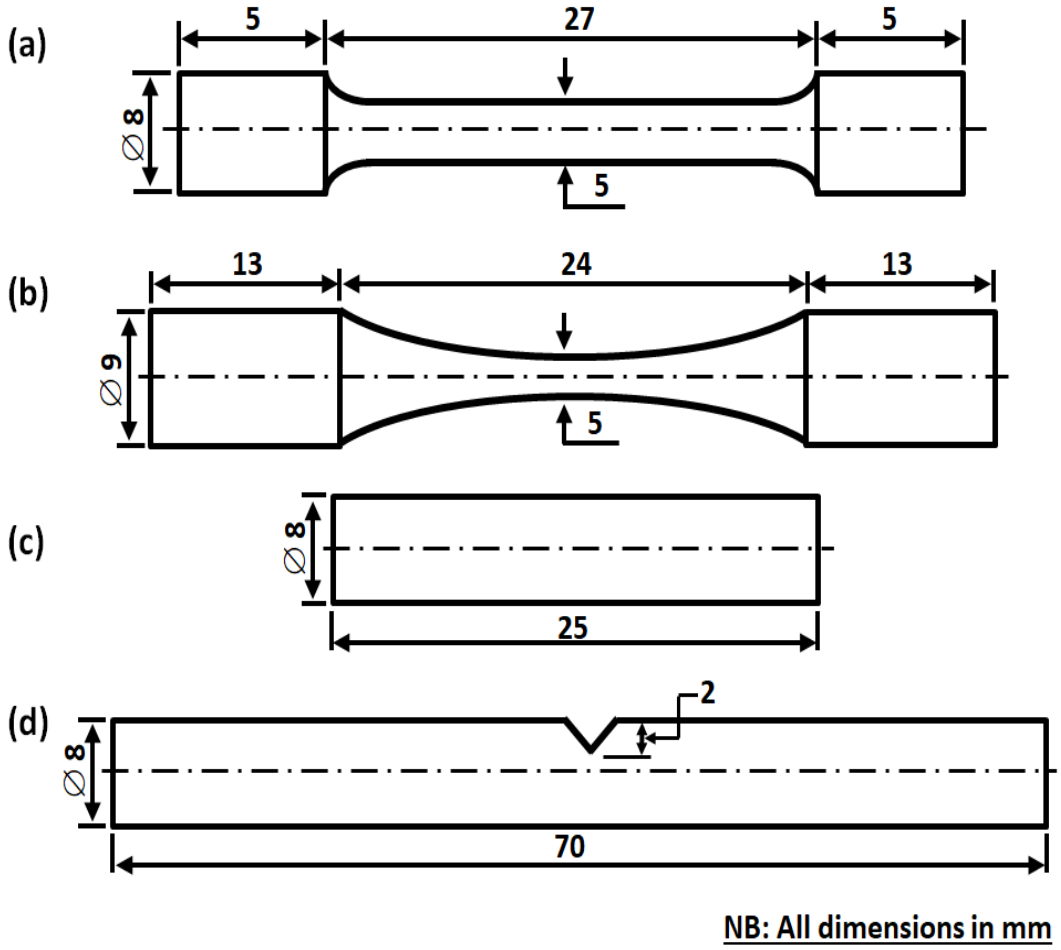

Fig. 1. Schematic diagrams of the machined (a) tensile; (b) fatigue; (c) compression and (d) impact tests specimens

2.7 Tensile Test

Tensile specimens with and without fibre reinforcement were respectively subjected to constant extension rate tensile (CERT) test on a Houndfield Tensometer in accordance with ASTM E-8 standard. As straining continued the ultimate uniaxial force applied on each specimen before fracture was recorded via a mercury column. Ultimate tensile strength was obtained by dividing the ultimate force with the original cross-sectional area of the specimen gauge section. Also, the percentage elongation-at-fracture of respective specimens was evaluated.

2.8 Compression Test

Using the same Tensometer, compression test was carried out according to ASTM E9-09 standard to obtain the maximum compression strength of the specimens with and without fibre reinforcement. The direction of loading on the specimens was opposite the direction exhibited in tensile test. Maximum compressive loads on the specimens were recorded and maximum compressive strength were then evaluated.

2.9 Fatigue Test

Fatigue test involves investigating the fatigue life of metals at fatigue stress amplitudes higher than and below the ultimate tensile strength of the metal. The fatigue limit (or endurance limit) is the fatigue stress below which failure will not occur after a very large number of loading cycles (i.e., infinite fatigue life). Fatigue limit (or endurance limit) is below ultimate tensile strength.

In accordance with ASTM Standard E606/E606-12, the fatigue properties of specimens were evaluated by clamping it on the grips of a completely reversed Avery Deninson 7305 Bending Fatigue Testing Machine with a zero mean stress. In total, thirteen test specifications were considered to accomodate series of stress amplitude loading in fatigue test. Hence, thirteen test pieces were machined for the respective specimen (i.e., for unreinforced specimen, and composite specimens with 0°, 30°, 60° and 90° fibre orientations).

Bending load was exerted on a test piece of unreinforced aluminium specimen by an oscillating spindle driven by a connecting rod, crank and double eccentric mechanism until a bending moment that corresponds to a maximum fatigue stress of amplitude of 950 MN/m^2 was attained. Tensile and compressive stresses were applied alternatively on the surface of the specimen as it was rotated under bending moment via a flexible coupling by a high-speed motor. A counter mounted on the motor recorded number of cycles (N) up to the number of cycles-to-failure (N_f). This procedure was repeated on other tets pieces of unreinforced specimen at decreasing stress amplitudes of 850, 750, 650, 550, 450, 350, 250, 200, 150, 100, 70, 50, 45, 40, 35 and 25 MN/m^2. However, testing was stopped after fatigue limit (or endurance limit) is established at a stess amplitude below the ultimate tesile strength of the specimen.

Similar tests were conducted on composite specimens with 0° (i.e., axial), 30°, 60° and 90° (i.e., transverse) fibre orientations. Like before, testing of identical specimens was stopped after fatigue limit (or endurance limit) is established at a stess amplitude below the ultimate tesile strength of the specimen. The fatigue stress amplitudes of specimens versus the number of cycles-to-failure were then plotted to obtain the S-N curve.

3. RESULTS AND DISCUSSION

The values of impact energy, percentage elongation-at-fracture, ultimate tensile strength and maximum compressive strength of the unreinforced aluminium alloy, and the variations with fibre orientation in reinforced aluminium composites are shown in Table 1.

The plot of impact energy versus the trend of fibre orientation is shown in Fig. 2. Unreinforced aluminium exhibits impact energy of 5.15 J; while deviation of fibre orientation from 0° to 30°, 60° and 90° causes impact energy to decrease from 8.68 to 5.56, 4.75 and 4.61 J, respectively.

The results show that aluminium composite specimens with 0° and 30° steel fibre orientations have more capacity to absorb impact deformation than the unreinforced specimen, and composite specimens with 60° and 90° steel fibre orientations. The highest impact enegy displayed by the composite specimen with 0° fibre orientation could be attributed to the the fact that the fibres offers continuous reinforcement spanning the longitudinal axis of the specimens. Also, the least impact enegy exhibited by the composite specimen with 90° fibre orientation could be attributed to the tranverse fibres offering areas of shear stress concentration at the fibre-matrix contacts assiting fibre-matrix debonding and crack propagation during the impact blow on the Izod Impact Testing Machine.

Table 1. Impact energy, percentage elongation-at-fracture, ultimate tensile strength and maximum compressive strength of unreinforced aluminium alloy and reinforced aluminium composites

Trend of Fibre orientation	Mechanical Properties			
	Impact Energy (J)	Percentage Elongation-at-Fracture (%)	Ultimate Tensile Strength (MN/m^2)	Maximum Compressive Strength (MN/m^2)
Unreinforced	5.15	15.88	72.56	231.13
0°-Fibre Orientation	8.68	24.58	132.70	310.66
30°-Fibre Orientation	5.56	17.91	89.17	251.06
60°-Fibre Orientation	4.75	12.20	63.67	226.91
90°-Fibre Orientation	4.61	11.87	60.34	209.93

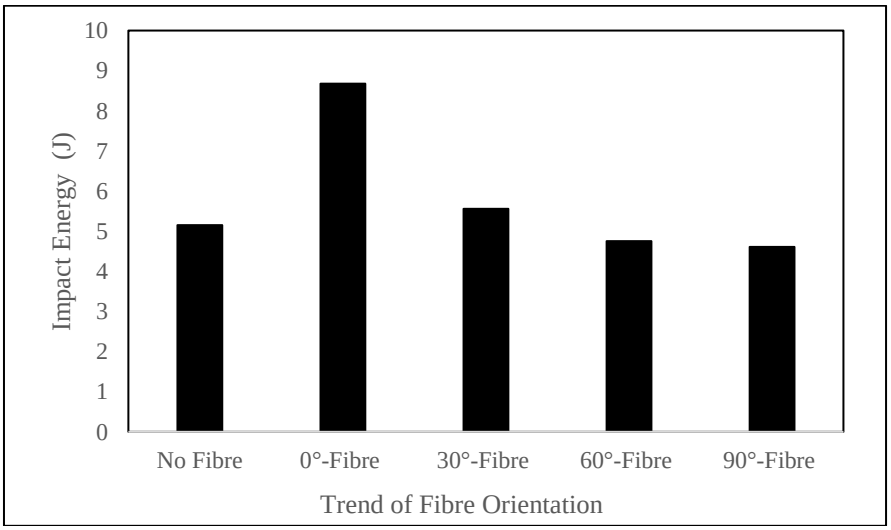

Fig. 2. Plot of impact energy versus trend of fibre orientation

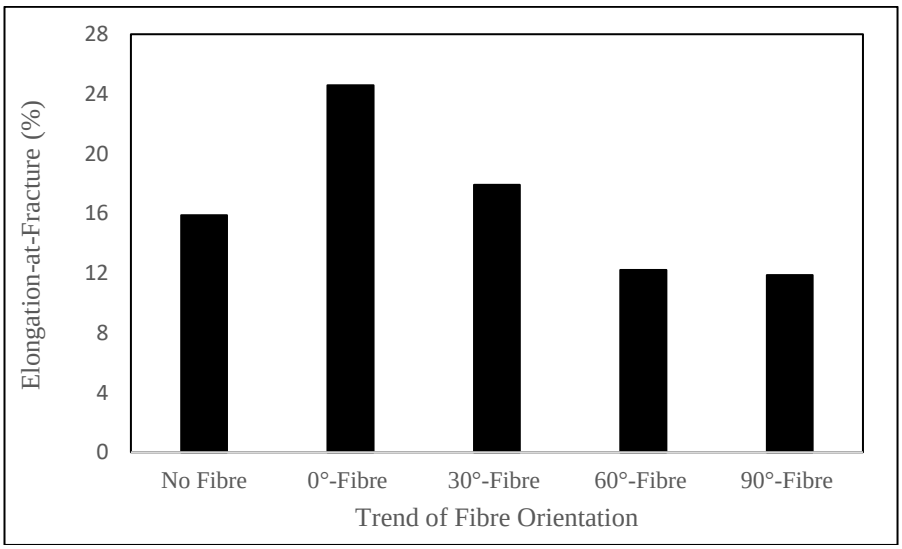

Fig. 3. Plot of percentage elongation-at-fracture versus trend of fibre orientation

Fig. 3 displays the variation of percentage elongation-at-fracture with the trend of fibre orientation. Percentage elongation-at-fracture of unreinforced aluminium is 15.88%. For fibre orientation from 0° to 30°, 60° and 90°, percentage elongation-at-fracture decreases from 24.58 to 17.91, 12.20 and 11.87%, respectively.

Composite specimen with 0° fibre orientation exhibited highest elongation-at-fracture (24.58%) because the axial fibres, being in the same direction of test, have the advantage of optimally enduring tensile loading before fracture on the Hounsfield Tensometer. However, the transverse fibres in the specimen with 90° fibre orientation offer remarkable stress concentration at fibre-matrix contacts causing debonding and crack propagation, thus offering the least endurance of tensile deformation before fracture as indicated by 11.87%.

The plot of ultimate tensile strength versus the trend of fibre orientation is shown in Fig. 4. Unreinforced aluminium exhibits ultimate tensile strength of 72.56 MN/m^2; while deviation of fibre orientation from 0° to 30°, 60° and 90° causes impact energy to decrease from 132.70 to 89.17, 63.67and 60.34 MN/m^2, respectively.

Here, similar trend occurs i.e., the longitunal fibres in specimen with 0° fibre orientation assist the specimen to offer optimal sustenance of tensile deformation before fracture as depicted by ultimate tensile strength of 132.70 MN/m^2, while the tranverse fibres in the specimen with 90° fibre orientation offer minimum sustenance of tensile deformation before fracture as indicated by 60.34 MN/m^2.

Fig. 5 displays the maximum compressive strength versus the trend fibre orientation.

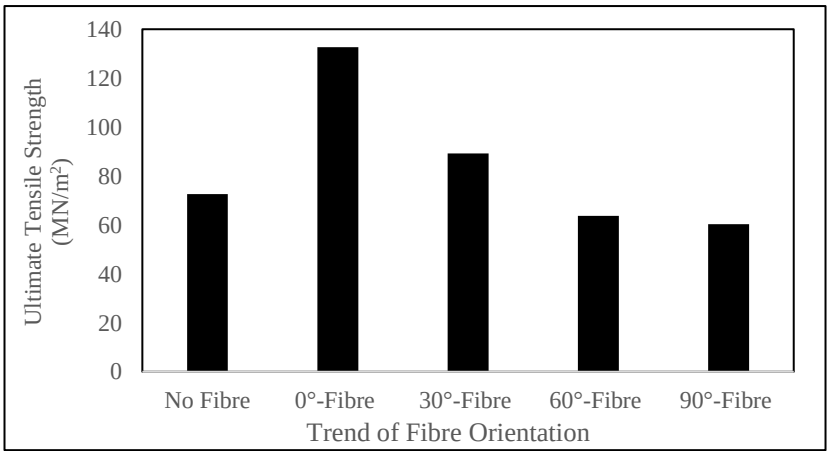

Fig. 4. Plot of ultimate tensile strength versus trend of fibre orientation

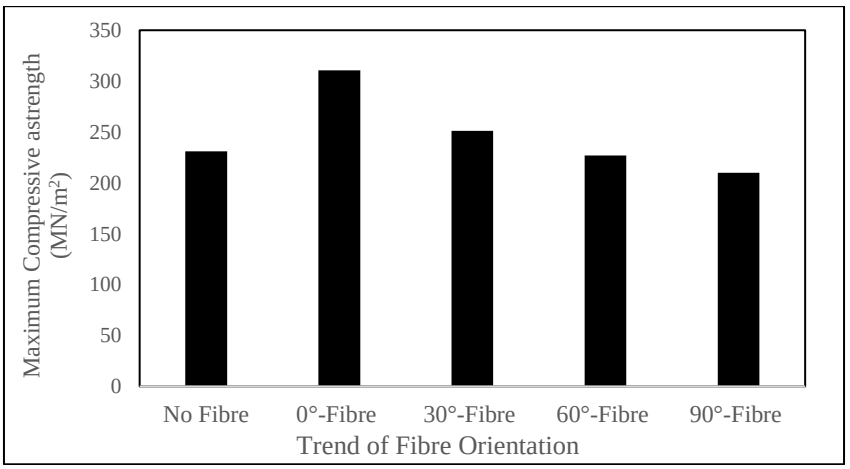

Fig. 5. Maximum compressive strength versus the trend fibre orientation

Unreinforced aluminium exhibits maximum compressive strength of 231.13 MN/m^2; while deviation of fibre orientation from 0° to 30°, 60° and 90° resulted in ultimate tensile strength decreasing from 310.66 to 251.06, 226.91 and 209.93 MN/m^2, respectively.

Composite specimen with 0° fibre orientation exhibiting highest compressive strength (310.66 MN/m^2) is attributed to the fact that the axial fibres offer more capacity of carrying the compressive load before fracture on the Hounsfield Tensometer. On the other hand, composite specimen with 90° fibre orientation offered the least compressive strength (209.93 MN/m^2) because of the negative effect of debonding and crack extension phenoma at the fibre-matrix contacts.

Table 2 shows the variations of fatigue stress amplitude with logarithmic scale of number of cycles-to-failure. The graphical representation of this is shown in Fig. 6.

At fatigue stress amplitude of 850 MN/m^2, the fatigue life of unreinforced aluminium specimen is 26 numbers of cycles-to-failure; while the deviation of fibre orientation from 0° to 30°, 60° and 90° yielded reduction in fatigue life from 64 to 36, 20 and 14 numbers of cycles-to-failure. At 650 MN/m^2 fatigue stress amplitude, the fatigue life of unreinforced aluminium specimen is 63 numbers of cycles-to-failure; while the deviation of fibre orientation from 0° to 30°, 60° and 90° yielded reduction in fatigue life from 106 to 83, 43 and 21 numbers of cycles-to-failure. Also, At fatigue stress amplitude of 250 MN/m^2, the fatigue life of unreinforced aluminium specimen is 505 numbers of cycles-to-failure; while the deviation of fibre orientation from 0° to 30°, 60° and 90° yielded reduction in fatigue life from 2741 to 861, 295 and 157 numbers of cycles-to-failure. Reduction in fatigue stress amplitude was found to increase the number of cycles-to-failure (i.e., the fatigue life) of the specimens.

The fatigue limit (or endurance limits) of unreinforeced aluminium, and aluminium composite having 0°, 30°, 60° and 90° fibre orientations are found to be 40, 70, 45, 35 and 25 MN/m^2, respectively. And the corresponding fatigue life are observed to be 35480, 199518, 112195, 10021 and 5297 numbers of cycles-to-failure.

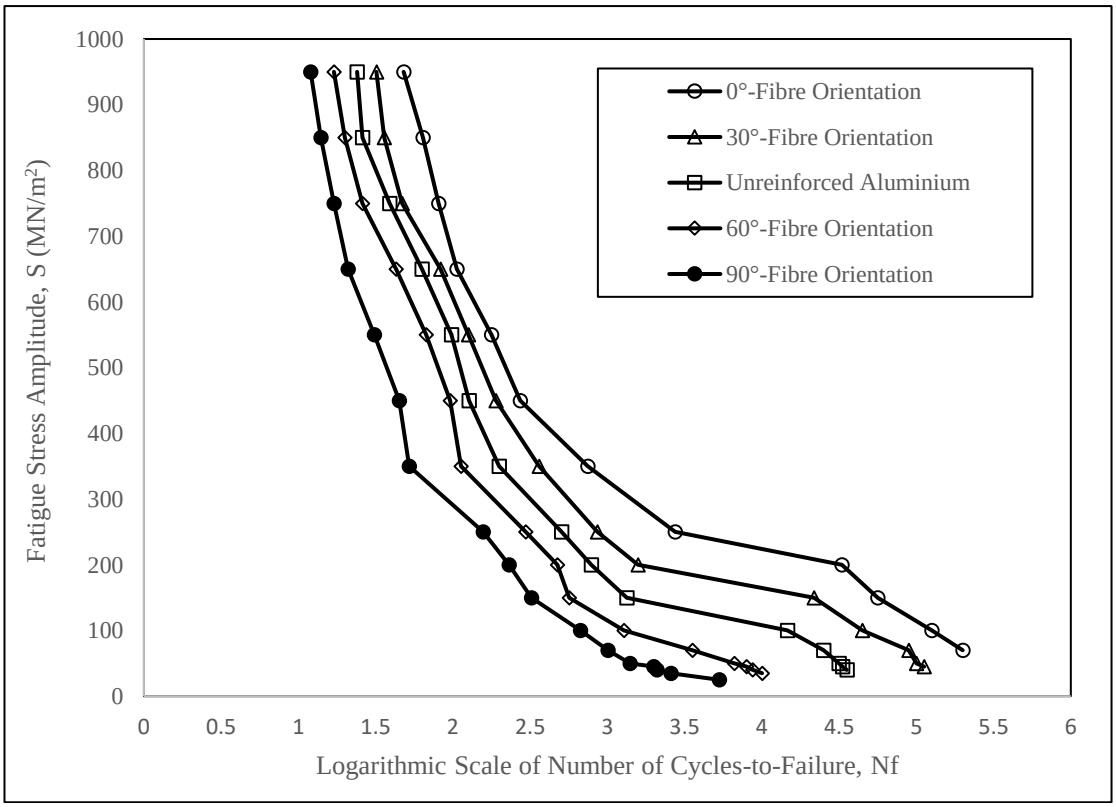

Fig. 6. Plot of fatigue stress amplitude versus logarithmic scale of number of cycles-to-failure for the specimens

Table 2. Variations of fatigue stress amplitude with logarithmic scale of number of cycles-to-failure

Fatigue Stress Amplitude, S (M/Nm^2)	Unreinforced Aluminium		0°-Fibre Orientation		30°-Fibre Orientation		60°-Fibre Orientation		90°-Fibre Orientation	
	N_f	log N_f	N_f	log N_f	N_f	log N_f	N_f	log N_f	N_f	log N_f
950	24	1.380	48	1.681	32	1.505	17	1.230	12	1.079
850	26	1.415	64	1.806	36	1.556	20	1.301	14	1.146
750	39	1.591	81	1.908	47	1.672	26	1.415	17	1.230
650	63	1.799	106	2.025	83	1.919	43	1.633	21	1.322
550	98	1.991	178	2.250	126	2.100	67	1.826	31	1.491
450	127	2.104	273	2.436	190	2.279	96	1.982	45	1.653
350	199	2.299	746	2.873	362	2.559	113	2.053	52	1.716
250	505	2.703	2741	3.438	861	2.935	295	2.470	157	2.196
200	785	2.895	32885	4.517	1577	3.198	475	2.677	231	2.364
150	1336	3.126	56238	4.750	21727	4.337	566	2.753	322	2.508
100	14622	4.165	125892	5.100	44668	4.650	1276	3.106	670	2.826
70	25118	4.400	199518	5.300	89125	4.950	3548	3.550	1008	3.003
50	31628	4.500	-	-	100024	5.000	6622	3.821	1403	3.147
45	33185	4.521	-	-	112195	5.050	7960	3.901	1992	3.300
40	35480	4.550	-	-	-	-	8706	3.940	2092	3.321
35	-	-	-	-	-	-	10021	4.001	2575	3.411
25	-	-	-	-	-	-	-	-	5297	3.724

The trends of fatigue and endurance limits show that composite specimens with 0° and 30° steel fibre orientations have more sustenance of fatigue deformation before failure than the unreinforced specimen, while the unreinforced specimen has more sustenance of fatigue deformation before faluire than the composite specimens with 60° and 90° steel fibre orientations.

The highest fatigue limit (or endurance limit) exhibited by the composite specimen with 0° fibre orientation could be attributed to fact that fact that the continuous spanning of the fibres in the axial dimension have maximum ability to sustain the applied alternating tensile and compressive stresses as it was rotated on the Avery Deninson 7305 Bending Fatigue Testing Machine. Also, the least fatigue limit (or endurance limit) displayed by the composite specimen with 90° fibre orientation could be attributed to remarkable stress concentration, debonding and crack growth at the tranverse fibre-matrix contacts.

4. CONCLUSION AND RECOMMENDATION

This work investigates the effect of steel fibres orientation on the anisotropic mechanical behaviour of aluminium composites. The mechanical properties evaluated are impact energy, tensile, compressive and fatigue properties.

The findings shows that specimen with 0° fibre orientations has maximum sustenance of deformation before fracture, followed by specimen with 30° fibre orientations, unreinforced specimen, specimens with 60° fibre orientation and 90° fibre orientation.

This could be attributed to the fact that the fibres in the composite with 0° fibre orientation offer continuous reinforcement spanning the longitudinal axis of the specimens, while fibre orientations from 30° to 90° offer areas of different degrees of shear stress concentration at fibre-matrix contacts aiding fibre-matrix debonding and crack propagation.

In conclusion, this work shows that orientation of steel fibre reinforcement in aluminium matrix could be varied to achieve ranges of mechanical properties and performances needed for different practical applications such as high-speed machineries, aircrafts and spacecrafts.

For future studies, the possibility of using other fibre materials apart from steel fibres for reinforcing aluminium alloy could be explored.

DISCLAIMER (ARTIFICIAL INTELLIGENCE)

Authors hereby declare that NO generative AI technologies such as Large Language Models (ChatGPT, COPILOT, etc.) and text-to-image generators have been used during the writing or editing of this manuscript.

COMPETING INTERESTS

Authors have declared that no competing interests exist.

REFERENCES

1. John VB. Introduction to Engineering Materials. 2nd Ed.: Macmillan Publishing Company Ltd; 1980.
2. Sigworth G. Understanding quality in aluminum castings. International Journal of Metalcasting. 2011;5(1):7-22.
3. Jorstad J, Apelian D. Hypereutectic Al-Si Alloys: Practical casting considerations. International Journal of Metal Casting. 2009;3(3):13-36.
4. Nam SW, Lee DH. Effect of mn on the mechanical behavior of al alloys, metals and materials. 2000;6:3-16. DOI.ORG/10.1007/BF03026339
5. Orozco-Gonzalez P, Castro-Roman M, López-Rueda J, Hernández-Rodríguez A, Muñiz-Valdez R, Luna-Álvarez S, Ortiz-Cuellar C. Effect of Iron Addition on the Crystal Structure of the α-Al-Fe-Mn-Si Phase Formed in the Quaternary Al-Fe-Mn-Si System. Revista de Metalurgia. 2011;47(6):453.
6. Li Z, Limodin N, Tandjaoui A, Quaegebeur P, Zhu X, Balloy D. Effect of Fe and Mn content on the microstructures and tensile behaviour of Al-Si7-Cu3 Alloy: Thermal Analysis and Tensile Test. Metals and Materials International. 2022;28:2118-2133.
7. Alawode AJ, Adeyemo SB. Mechanical properties of cast aluminium rods under varied foundry sand sizes and mould preheat temperatures. Journal of Engineering and Applied Sciences. 2008;3(8):626-633.
8. Isadare D, Aremo B, Adeoye MO, Olawale O. Effect of heat treatment on some mechanical properties of 7075 Aluminium

Alloy. Materials Research. 2013;16(1):190-194.
DOI:10.1590/S151614392012005000167

9. Ding L, Jia Z, Zhang Z, Sanders R, Liu Q, Yang G. The natural aging and precipitation hardening behaviour of Al-Mg-Si-Cu Alloys with different Mg/Si ratios and Cu Addition. Materials Science and Engineering. 2015;627:119-126.
DOI:10.1016/J.MSEA.2014.12.086
10. Aliyah AN, Anawati A. Effect of heat treatment on microstructure and mechanical hardness of aluminum alloy AA7075. IOP conference series: Materials Science and Engineering. 2019;541 012007.
11. Mahan HM, Konovalov SV, Panchenko I. Effect of heat treatment on the mechanical properties of the aluminium alloys AA2024 with Nanoparticles, International Journal of Applied Science and Engineering. 2023; 20(2):1-6.
DOI:
DOI/10.6703/IJASE.202306_20(2).011
12. Geofrey TMT, Goodwin PS, Ward-Close CM. Titanium Particulate Metal Matrix Composites-Reinforcement, Production Methods, and Mechanical Properties. Advanced Engineering Materials. Wiley Online Library; 2000.
13. Mitrović S, Babić M, Stojanović B, Miloradović N, Pantić M, Džunić D. Tribological potential of hybrid composites based on zinc and aluminium alloys reinforced with SiC and graphite particles. Tribology in Industry. 2012;34(4):177-185.
14. Alaneme KK, Bamike BJ. Characterization of mechanical and wear properties of aluminium based composites reinforced with quarry dust and silicon carbide. Ain Shams Engineering Journal. 2018;9(4): 2815-2821.
15. Yang Z, Fan J, Liu Y, Yang Z, Kang Y, Nied J. Effect of combination variation of particle and matrix on the damage evolution and mechanical properties of particle reinforced metal matrix composites. Materials Science and Engineering. 2021;806.
16. Wang Y, Monetta T. Systematic study of preparation technology, microstructure characteristics and mechanical behaviors of SiC Particle-Reinforced metal matrix composite. Journal of Materials Research and Technology. 2023;25:7470-7497.
17. Huang Z, Qian X, Su Z, Pham DC, Sridar N. Experimental investigation and damage simulation of large-scaled filament wound composite pipes, composites part B: Engineering. 2020;184.
18. Qui Z, Liu Q, Un Y, Li Q. On Crushing responses of filament winding CFRP/Aluminum and GFRP/CFRP/Aluminum hybrid structures. Composites Part B: Engineering. 2020;200.
19. Stephen JT, Alawode AJ, Adegoke SO. Investigating the mechanical properties of cast aluminium rods reinforced with wet filament winding. International Journal of Research and Scientific Innovation. 2021;9(1):1-8.
20. Harmon DM, Saff CR. Damage Initiation and growth in fiber-reinforced metal matrix composites. ASTM Selected technical papers on metal matrix composites: Testing, Analysis, and Failure. 1989; 1032:237-250.
21. Aboudi J, Pindera MJ, Arnold SM. Thermoelastic Response of metal matrix composites with large-diameter fibers subjected to thermal gradients. NASA TM. 1993;106344.
22. Nguyen TB, Jeng SM, Yang JM. The effect of fibre orientation on fatigue crack propagation in SCS-6/Ti-15-3 composites. Materials Science and Engineering A. 1994;183(1-2):1-9.
DOI: 10.1016/0921-5093(94)90884-2.
23. Chen H, Alpas AT. Wear of aluminium matrix composites reinforced with nickel-coated carbon fibres. Wear. 1996;192(1-2):186-198.
24. Sanders BP, Mall S, Jackson SC. Load ratio effect on fatigue response of titanium matrix composites at elevated temperature. International Journal of Fatigue. 1999;21(2):121-134.
25. Peng HX, Fan Z, Mudher DS, Evans JRG. Microstructures and mechanical properties of engineered short fibre-reinforced aluminium matrix composites. Materials Science and Engineering: A. 2002;335(1-2):207-216.
DOI: 10.1016/S0921-5093(01)01930-X
26. Prasad SV, Asthana R. Aluminium metal-matrix composites for automotive applications: tribological considerations. Tribology Letters. 2004;17:445-453.
DOI:10.1023/B:TRIL.0000044492.91991.F3

27. Abhilash E, Joseph MA. Carbon fibre reinforced aluminum matrix composite: Development and evaluation of mechanical behaviors. proceedings of the international conference on materials science and technology. Pittsburgh, Pennsylvania. 2008;2577-2586.
28. Agbanigo AO, Alawode AJ. Evaluating the mechanical properties of aluminium-based composites reinforced with steel fibres of different orientations. Journal of Engineering and Applied Sciences. 2008; 3(12):933-936.
29. Periasamy M, Manickam B, Hariharasubramanian K. Impact properties of aluminium glass-fiber reinforced plastics sandwich panels. Materials Research. 2012;15(3):347-354.
DOI: 10.1590/S1516-14392012005000036
30. Pinto JW, Sujaykumar G, Sushiledra RM. Effect of heat treatment on mechanical and wear characterization of coconut ash and E-Glass Fiber-Reinforced aluminium hybrid composites. American Journal of Material Science. 2016;6(4A): 15-19.
DOI: 10.5923/C.MATERIALS.201601.03.
31. Nanjan S, Janakiram GM. Characteristics of A6061/(Glass Fibre + AL2O3 + SiC + B4C) reinforced hybrid composite prepared through STIR casting. Advances in Materials Science and Engineering. 2019;1-12.
32. Yogesh S, Madhu S. Mechanical properties evaluation of Al reinforced CFRP fiber metal laminate. Materials Today: Proceedings. 2020;33(1):44-47.
33. Mahaviradhan N, Sivaganesan S, Sravya NP, Parthiban A. Experimental investigation on mechanical properties of carbon fiber reinforced aluminum metal matrix composite. Materials Today: Proceedings. 2021;39(1):743-747.
34. Ba Y, Sun S. Tensile, Fatigue properties of fiber-reinforced metal matrix composites Cf/5056 Al. Composites and Advanced Materials. 2021;30:1-7.
35. Narayana SL, Gopalan V. Investigations on mechanical properties of jute fibre reinforced with aluminium oxide fortified epoxy composite. Advances in Materials and Processing Technologies. 2023;9(3): 779-804.
36. Abdulqadir SF, Alaseel BH, Sameer JO. Comparison of the mechanical properties and approach to numerical modeling of fiber-reinforced composite, high-strength steel and aluminum. Journal of Engineering and Technological Sciences. 2024;56(1):110-124.
DOI:DOI/10.5614/J.ENG.TECHNOL.SCI.2023.56.1.9

Disclaimer/Publisher's Note: The statements, opinions and data contained in all publications are solely those of the individual author(s) and contributor(s) and not of the publisher and/or the editor(s). This publisher and/or the editor(s) disclaim responsibility for any injury to people or property resulting from any ideas, methods, instructions or products referred to in the content.

© Copyright (2024): Author(s). The licensee is the journal publisher. This is an Open Access article distributed under the terms of the Creative Commons Attribution License (http://creativecommons.org/licenses/by/4.0), which permits unrestricted use, distribution, and reproduction in any medium, provided the original work is properly cited.

Peer-review history:
The peer review history for this paper can be accessed here:
https://www.sdiarticle5.com/review-history/124431